

# Scattering optics of snow

Alexander A. Kokhanovsky and Eleonora P. Zege

Permanent snow and ice cover great portions of the Arctic and the Antarctic. It appears in winter months in northern parts of America, Asia, and Europe. Therefore snow is an important component of the hydrological cycle. Also, it is a main regulator of the seasonal variation of the planetary albedo. This seasonal change in albedo is determined largely by the snow cover. However, the presence of pollutants and the microstructure of snow (e.g., the size and shape of grains, which depend also on temperature and on the age of the snow) are also of importance in the variation of the snow's spectral albedo. The snow's spectral albedo and its bidirectional reflectance are studied theoretically. The albedo also determines the spectral absorptance of snow, which is of importance, e.g., in studies of the heating regime in snow. We investigate the influence of the nonspherical shape of grains and of close-packed effects on snow's reflectance in the visible and the near-infrared regions of the electromagnetic spectrum. The rate of the spectral transition from highly reflective snow in the visible to almost totally absorbing black snow in the infrared is governed largely by the snow's grain sizes and by the load of pollutants. Therefore both the characteristics of snow and its concentration of impurities can be monitored on a global scale by use of spectrometers and radiometers placed on orbiting satellites.

© 2004 Optical Society of America

OCIS codes: 290.0290, 290.4020, 290.1990, 290.4210, 290.7050, 280.0280.

## 1. Introduction

Snow covers a large portion of the terrestrial surface during the winter season. Therefore snow fields have potentially significant effects on the planetary albedo and climate. The main factors in the influence of snow fields are snow cover and snow albedo  $r$ . Snow is highly reflective in the visible, where the solar spectrum's maximum is located. Then albedo  $r$  is close to 1. However, the albedo decreases in the UV and IR spectral regions. The decrease in albedo is the most pronounced in the near-IR spectral region, with values of  $r$  close to zero at 1.5, 2.0, and 2.5  $\mu\text{m}$ , where ice absorption maxima are located. Snow is essentially black then.

The snow's albedo controls the surface energy budget and the rate of melting. Therefore, knowledge of the albedo helps in understanding the seasonal

change in snow cover. A large amount of both experimental and theoretical research is devoted to studies of snow's optical properties. Recent comprehensive reviews<sup>1,2</sup> contain ~300 references to the subject. One of the most important results that was found is the fact that snow's spectral albedo can be fitted by radiative transfer calculations under the assumption of spherical shape of snow grains<sup>3–5</sup> (see, e.g., Fig. 10 of Ref. 4 and Fig. 9 of Ref. 5). This fact has allowed algorithms for retrieval of snow's grain size from airborne and spaceborne optical instruments to be developed.<sup>1,6</sup>

It is known, however, that snow *in situ* has an extremely complex structure and consists of irregularly shaped ice grains in contact with one another (see, e.g., Fig. 5 of Ref. 2). The optical properties of particles are controlled not only by the size but also by the shape of the particles.<sup>7,8</sup> Therefore it is clear that the model of spherical particles has a limited applicability to snow optics. An examination of this physical problem is the main task of this paper. Note that some important advances in this direction have already been reported.<sup>9</sup> In particular, it was shown<sup>9</sup> that the actual shape of grains has a profound effect on snow's bidirectional reflectance in the visible. Another issue that is addressed in this paper is the influence of close-packed effects<sup>10</sup> on snow's reflective properties.

According to our main ideas about snow optics that

A. A. Kokhanovsky (alexk@iup.physik.uni-bremen.de) is with the Institute of Environmental Physics, Bremen University, Otto Hahn Allee 1, D-28213 Bremen, Germany, and the B. I. Stepanov Institute of Physics, National Academy of Sciences of Belarus, 70 Skarina Avenue, 220072 Minsk, Belarus. E. P. Zege is with the B. I. Stepanov Institute of Physics, National Academy of Sciences of Belarus, 70 Skarina Avenue, 220072 Minsk, Belarus.

Received 4 June 2003; revised manuscript received 31 October 2003; accepted 31 October 2003.

0003-6935/04/071589-14\$15.00/0

© 2004 Optical Society of America

are developed in detail in this paper, the snow optics should be constructed with use of the following:

- A model of snow as fractal close-packed ice grains instead of a noninteractive spheres as in the conventional spherical model,
- Simple geometrical optics equations instead of Mie calculation for the snow's local optical characteristics; and
- Special exponential, analytical, asymptotic solutions of the radiative transfer theory for global snow's optical properties instead of computations with radiative transfer codes.

Implementation of these ideas provides simple analytical solutions and analytical comprehensive algorithms for retrieval of snow's grain size and pollution concentration. Such an approach has been developed and carefully tested but poorly publicized until now. The main ideas of this approach were discussed in several workshops on the retrieval techniques for the Global Imager instrument developed by the National Space Development Agency of Japan in 1996, 1997, and 1998.

In this paper we give a comprehensive pattern of this new approach to snow optics. The paper is organized as follows: In Section 2 we discuss snow's global optical characteristics such as spherical and plane albedos. The approximate formula for snow's bidirectional reflectance is also given there. Section 3 is devoted to studies of snow's local optical characteristics (e.g., transport and absorption path lengths). The problem of determining snow's grain size from reflectance spectroscopy data is considered in Section 4.

## 2. Global Optical Characteristics of Snow

### A. General Equations

Size  $d$  of snow grains is usually close to 1 mm.<sup>2</sup> This means that the methods of geometrical optics<sup>8,11,12</sup> can be applied to studies of snow's local optical characteristics in the visible and the near IR. It is easy to show that the photon free-path length in snow,  $l$ , in the spectral range considered is close to the value of  $d$ :  $\lambda \ll l \sim d$ .<sup>12</sup>

The radiative transfer equation cannot be applied if  $\lambda \gg l$ .<sup>13</sup> Then the simple geometrical optics scheme that lies at the very heart of the radiative transfer theory would no longer be applicable. As we shall see, such is fortunately not the case for snow in the visible and the near IR. Therefore we assume that the radiative transfer equation can be used for calculating snow's radiative characteristics.

In particular, we use the following approximate analytical solution of this equation, which is valid in the limit of small absorption<sup>14,15</sup>:

$$R(\mathbf{q}) = R_0(\mathbf{q}) \exp[-\alpha f(\mathbf{q})]. \quad (1)$$

Here  $R$  is the bidirectional reflectance (or the reflection function<sup>16</sup>) of a semi-infinite snow layer.

Vector-parameter  $\mathbf{q}$  has coordinates  $\vartheta_0$ ,  $\vartheta$ , and  $\varphi$ , which are the incident zenith angle, the observation zenith angle, and the relative azimuth, respectively.

The function  $f(\mathbf{q})$  in Eq. (1) is given by the following ratio<sup>15</sup>:

$$f(\mathbf{q}) = \frac{K_0(\vartheta_0) K_0(\vartheta)}{R_0(\vartheta_0, \vartheta, \varphi)}, \quad (2)$$

where  $R_0$  equals the value of  $R$  at zero absorption and<sup>12</sup>

$$K_0(\vartheta_0) = \frac{3}{4} \cos \vartheta_0 + \frac{3}{4\pi} \int_0^{2\pi} d\varphi \int_0^{\pi/2} \times R_0(\vartheta_0, \vartheta, \varphi) \cos^2 \vartheta \sin \vartheta d\vartheta. \quad (3)$$

The function  $K_0(\vartheta_0)$  is called the escape function in radiative transfer theory. It determines the angular distribution of light escaping from the semi-infinite nonabsorbing medium in the framework of the Milne problem (with sources located at infinity inside a medium<sup>16</sup>).

We also have for  $\alpha$  in Eq. (1) (Ref. 12)

$$\alpha = 4 \sqrt{l_{\text{tr}}/3l_{\text{abs}}}, \quad (4)$$

where  $l_{\text{abs}}$  is the absorption path length and  $l_{\text{tr}}$  is the transport path length. Studies of the accuracy of Eq. (1) compared with the solution of the radiative transfer equation can be found in Refs. 17 and 18. Equation (1) can be applied with high accuracy for values of  $\alpha$  less than unity.

Note that the phase coherence of scattered light is lost over length scales that are longer than  $l_{\text{tr}}$ . The path of a scattered photon can be then described as a random walk with step size  $l_{\text{tr}}$ . On length scales that are long compared with  $l_{\text{tr}}$  it is useful to regard this random walk as photon diffusion with diffusion coefficient  $D = v l_{\text{tr}}/3$ , where  $v$  is the speed of light in the medium. Therefore  $l_{\text{tr}}$  is an important parameter of our theory. The value of  $l_{\text{abs}}$  is the length scale at which absorption effects become important. This parameter is large in the visible range of the electromagnetic spectrum. However, it rapidly decreases with wavelength owing to stronger light absorption by ice in the near-IR region. In fact, only these two parameters of a scattering medium enter into the light-diffusion equation.<sup>12</sup>

We have from Eq. (1), as  $\alpha \rightarrow 0$ ,

$$R(\mathbf{q}) = R_0(\mathbf{q}) - \alpha K_0(\vartheta_0) K_0(\vartheta), \quad (5)$$

which is a familiar result of the radiative transfer theory.<sup>16</sup> Equation (5) allows us to establish the physical meaning of  $\alpha$ . That is, by performing the integration with respect to  $\vartheta_0$ ,  $\vartheta$ , and  $\varphi$  we obtain from Eq. (5) for the spherical albedo<sup>19</sup>

$$r = 1 - \alpha, \quad (6)$$

where we have used Eq. (3) and the energy conservation law [see Eq. (A5) in Appendix A]. Recall that spherical albedo  $r$  is defined as<sup>16</sup>

$$r = \frac{2}{\pi} \int_0^{2\pi} d\varphi \int_0^1 \xi d\xi \int_0^1 \eta d\eta R(\xi, \eta, \varphi), \quad (7)$$

where we have introduced the cosines  $\xi = \cos \vartheta_0$  and  $\eta = |\cos \vartheta|$ .

The value of  $r$  gives the fraction of light energy reflected from a semi-infinite medium under diffuse illumination. The value of  $\alpha$  is, therefore, the fraction of the absorbed energy at the same conditions (and  $r$  close to unity). It follows [see Eq. (4)] that media with more absorbing particles (smaller  $l_{\text{abs}}$ ) do not necessarily give the largest absorption by a medium as a whole. Instead, it is the ratio  $Z = l_{\text{tr}}/l_{\text{abs}}$  that is of importance. In particular, different semi-infinite weakly absorbing disperse media that have the same values of  $Z$  have values similar to reflectances  $R(\mathbf{q})$ , provided that functions  $R_0(\mathbf{q})$  are close as well. The physical reason for this fact is quite clear. Indeed, it is not only the absorption by a local volume that matters but also the type of scattering diagram. In particular, scattering diagrams that are highly extended in the forward direction with large values of  $l_{\text{tr}}$  lead also to a larger number of scattering and absorption events (hence, to a larger probability of absorption by a medium as a whole) before the escape of photons from the medium.

## B. Escape Function

Let us consider escape function  $K_0(\vartheta)$  [Eq. (3)] in more detail now. It follows from the general radiative transfer theory that the function  $K_0(\vartheta)$  describes the angular distribution of light emerging from a semi-infinite nonabsorbing layer with light sources placed at an infinite depth inside the medium (the Milne problem).<sup>20,21</sup> This means, in particular, that this function should not depend strongly on the type of scatterer. Such a property of the function  $K_0(\vartheta)$  is confirmed by numerical calculations.<sup>19,21</sup> In particular, the following approximation can be used for all types of scatterer<sup>22</sup>:

$$K_0(\xi) = (3/7)(1 + 2\xi) \quad (8)$$

if  $\xi \geq 0.2$ .<sup>12,15,22</sup> Equation (8) is not influenced by a particular single-scattering law and can be used for media of various types, including snow.

We emphasize that Eq. (8) also describes the angular distribution of light transmitted by thick layers of snow.<sup>12</sup> This suggests a simple way for experimental verification of Eq. (8) (e.g., performing angular measurements of transmitted light in a cold chamber). Such data are not available to us. So we have chosen an indirect way to check Eq. (8) as applied to snow optics, as follows.

One can obtain from Eq. (1) for a plane albedo  $r_p(\xi)$  (Appendix A)

$$r_p(\xi) = \exp[-\alpha K_0(\xi)], \quad (9)$$

where  $r_p(\xi)$  is defined as

$$r_p(\xi) = \frac{1}{\pi} \int_0^{2\pi} d\varphi \int_0^1 R(\xi, \eta, \varphi) \eta d\eta. \quad (10)$$

A similar equation can be derived for the spherical albedo given by Eq. (7) (Appendix A). It follows that  $r = \exp(-\alpha)$ .

The quantity  $r_p(\xi)$  has been measured by many authors (see, e.g., Refs. 4, 23, and 24). It follows from Eq. (9) that

$$K_0(\xi) = \frac{1}{\alpha} \ln \frac{1}{r_p(\xi)}. \quad (11)$$

The precise value of  $\alpha$  is usually unknown for a given experiment. However,  $\alpha$  does not depend on  $\xi$ .

Let us define the normalized escape function  $K_{0n}(\xi) = K_0(\xi)/K_0(\xi^*)$ . Then it follows from Eq. (8) that

$$K_{0n}(\xi) = \frac{1 + 2\xi}{1 + 2\xi^*}, \quad (12)$$

where  $\xi^*$  is a cosine of the selected incidence angle. We assume that  $\xi^* = 0.7$ . Clearly, any other value of  $\xi^* > 0.2$  [see Eq. (8)] can be used for the normalization. It follows from Eq. (11) that

$$K_{0n}(\xi) = \frac{\ln r_p(\xi)}{\ln r_p(\xi^*)}. \quad (13)$$

Therefore, measurements of  $r_p(\xi)$  can be used to establish the relative angular dependence of the function  $K_0(\xi)$ . The remaining proportionality constant can easily be found from the condition

$$2 \int_0^1 K_0(\xi) \xi d\xi = 1, \quad (14)$$

which follows from the energy conservation law.<sup>19</sup>

A comparison of the function  $K_{0n}(\xi)$  derived from Eq. (12) at  $\xi^* = 0.7$  and of measurements of  $r_p(\xi)$  [Eq. (13)] is given in Fig. 1. We can see that the experimental data closely follow the approximation in the range  $\xi \geq 0.4$ . The difference between curves can be attributed in particular to the inaccuracy related to taking experimental data from plots  $r_p(\xi)$  (especially at  $\xi < 0.4$ , where  $r_p$  is close to 1). We also show the results of the exact calculation<sup>21</sup> of the function  $K_{0n}(\xi)$  for media characterized by the Heney–Greenstein (HG) phase function  $p(\theta) = \sum_{l=0}^{\infty} g^l P_l(\cos \theta)$  in Fig. 1. Here  $P_l(\cos \theta)$  is a Legendre polynomial. It is assumed that  $g = 0.75$ . Note that  $p(\theta)$  gives the probability of photon scattering in the direction specified by scattering angle  $\theta$  and that  $g = \frac{1}{2} \int_0^\pi p(\theta) \sin \theta \cos \theta d\theta$  is the asymmetry parameter.

Aoki *et al.*<sup>5</sup> found that the HG phase functions are more suitable than Mie phase functions for studies of snow's optical properties. It should be stressed, however, that the function of  $K_0(\xi)$  is highly robust to variations in phase function [at least for  $\xi \geq 0.2$  (Ref. 19)]. The exact result and the approximation in Fig.

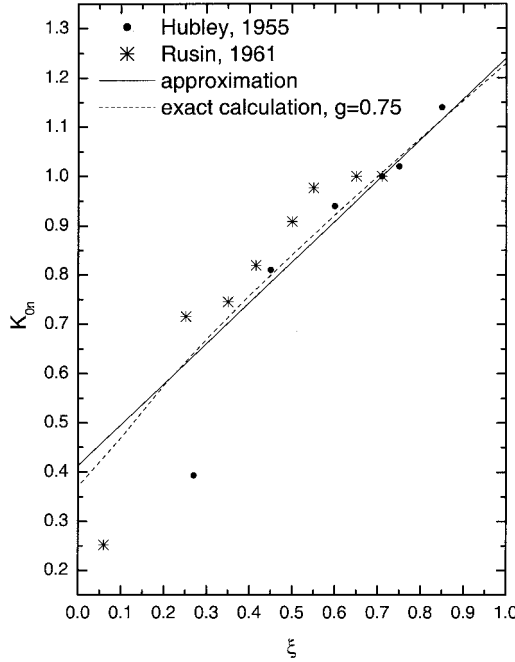


Fig. 1. Dependence of the normalized escape function on the cosine of the incidence angle according to measurements in Refs. 23 and 24, Eq. (12), and the exact calculations<sup>21</sup> for the HG phase function with  $g = 0.75$ .

1 are in close correspondence at  $\xi \geq 0.2$  (the error is less than 2%). Therefore we conclude that Eq. (8) can be used in conjunction with Eqs. (1) and (2) for studying the influence of absorption on the bidirectional reflectance of snow. Note that  $K_0(\xi)$  increases with  $\xi$ ; this leads to a decrease of  $r_p$  with  $\xi$  [Eq. (9)], as has been confirmed by field measurements.<sup>4,23,24</sup>

We can see, therefore, that the plane albedo of snow is larger for the Sun at the horizon (small values of  $\xi$ ) than for the overhead Sun. The physics behind this effect is quite transparent. Indeed, photons injected into the medium along slant paths have more chances to survive than those at perpendicular incidence.

### C. Bidirectional Reflectance

To model the bidirectional reflectance function of a plane-parallel semi-infinite snow layer  $R(\mathbf{q})$  we should also know function  $R_0(\mathbf{q})$  for nonabsorbing snow [Eqs. (1) and (2)]. That function depends on phase function  $p(\theta)$  only. Various assumptions about function  $p(\theta)$  (see, e.g., Refs. 25–31) lead to diverse results as far as function  $R_0(\mathbf{q})$  is concerned. This fact was clearly demonstrated in Ref. 9 (see Fig. 5 of Ref. 9) for three shapes of particles, namely, spheres, hexagonal cylinders, and fractals (see also Fig. 2 of this paper). Therefore it is of importance to make the correct selection of the phase function in modeling the bidirectional reflectance of snow.

Several theoretical phase function models are given in Fig. 3, together with experimental data<sup>25</sup> for a crystalline disperse medium. The spherical model should be rejected. In particular, if this model were

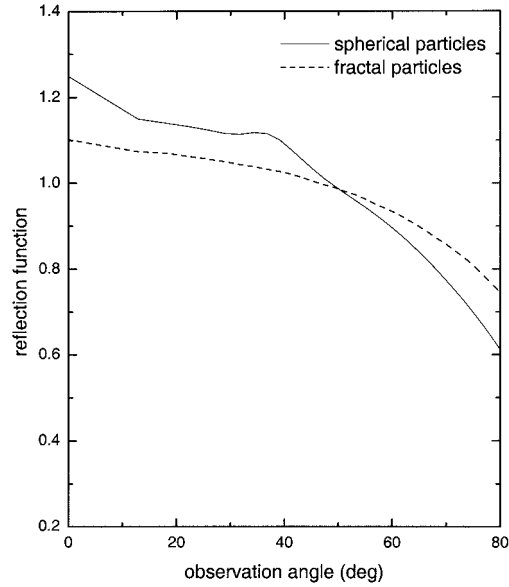


Fig. 2. Reflection functions of a semi-infinite nonabsorbing medium with spherical and fractal grains at nadir illumination as a function of observation angle. Calculations were performed by use of the radiative transfer code described in Ref. 9 for a refractive index  $n$  equal to 1.31 and a wavelength equal to 0.55  $\mu\text{m}$ . The model of fractal particles that we used is described in Ref. 29. A size distribution of spherical particles is given by the cloud model C.1 with effective radius  $a_{\text{ef}} = 6 \mu\text{m}$  (Ref. 12) and a coefficient of variance of the particle size distribution equal to  $7^{-1/2}$ . The increase in the size of the particles has an insignificant influence on the results.<sup>19</sup>

valid, rainbows and glories should be observed (see the solid curve in Fig. 3 at scattering angles  $\theta$  close to  $145^\circ$  and  $180^\circ$  and the solid curve in Fig. 2 for angles at  $35^\circ$  and  $0^\circ$ ). Clearly, this model is not valid for snow. The hexagonal cylinder model studied in Ref. 9 should also be rejected because such shapes do not appear in snow in large numbers.<sup>2</sup>

The random particle model<sup>26,27</sup> and the fractal-particle model<sup>28,29</sup> are good candidates for modeling bidirectional reflectance, however. The first model is based on the distortion of a spherical shape by the Gaussian distribution of its surface with various parameters. The fractal particle is constructed in the following way: The initial shape is a regular tetrahedron. A part of its surface is replaced by a reduced version of the same tetrahedron. The repetition of this procedure at smaller triangles leads to a fractal surface with the dimension  $\ln 6/\ln 2 \approx 2.58$ .<sup>29</sup> Further details of the stochastic-particle models and the numerical procedures for finding  $p(\theta)$  can be found in Refs. 26–30.

We stress that functions  $p(\theta)$  for fractals<sup>28,29</sup> and random particles<sup>26,27</sup> are similar (Fig. 3). Therefore functions  $R_0(\mathbf{q})$  for fractals and for random particles do not differ much. This fact underlines the fact that what is of importance is not the particular stochastic particle model but rather the level of randomness in a given model.<sup>8</sup>

We choose the fractal model here because it has no

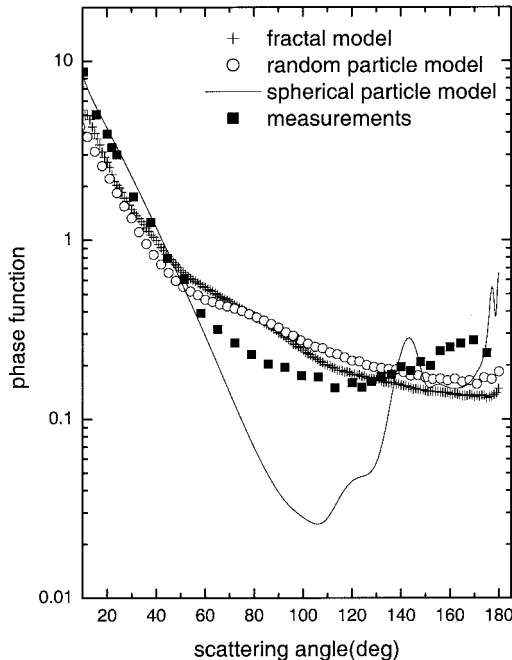


Fig. 3. Phase functions of ice particles for various theoretical models and measurements.<sup>25</sup> Calculations were performed with the geometrical optical approximation at the wavelength  $0.55 \mu\text{m}$ , where absorption of light by ice is extremely weak. The fractal-particle model is described in Ref. 29. The random-particle model is described in Ref. 26. A standard deviation of  $\sigma = 0.2$  and correlation angle  $\Gamma = 5^\circ$  were assumed for calculations according to the random-particle model.<sup>26</sup> The sizes of the particles in fractal- and random-particle models do not influence the results given here. The phase function for spherical particles was calculated for the same spherical polydispersion as for Fig. 2 but for the effective radius  $a_{\text{ef}} = 15 \mu\text{m}$ .

free parameters for nonabsorbing ice particles and corresponds closely to the random-particle model<sup>26</sup> at extreme values of its randomness parameters.<sup>26,27</sup> The final decision, however, should be made when measurements of the snow's phase function *in situ* are performed.

It should be stressed that the poor correspondence of measurements and the theory for fractals near  $90^\circ$  and  $170^\circ$  (Fig. 3) could be due to the presence of small crystals or even of ice spheres in the experiment<sup>25</sup> (see the photomicrograph in Ref. 25). The authors of Ref. 25 have been able to describe their experimental curve with high precision by using the unified theory of light scattering by ice crystals, assuming the following shapes of crystals: irregular bullet rosettes and plates with rough surfaces. Clearly, the combination of different shapes can be used to model observed phase functions of crystalline disperse media with a high accuracy.<sup>31</sup> However, here the problem of the uniqueness arises. Therefore we prefer to use a model of a single randomly oriented fractal particle, which has no free parameters attached.

A comparison of measurements<sup>32</sup> of  $R(\vartheta)$  at  $\vartheta_0 = 0^\circ$  and calculations that use Eq. (1) with Eq. (8) taken into account and function  $R_0$  given in Fig. 2 for fractal

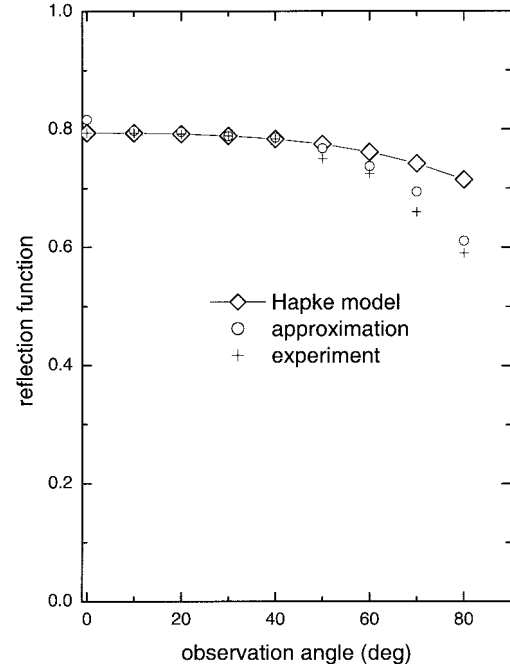


Fig. 4. Reflection function of snow obtained from measurements<sup>32</sup> made according to our approximation [Eq. (1)] and Hapke's model.

particles is shown in Fig. 4. The value of  $\alpha$  was not specified in the experiment.<sup>32</sup> So we used  $\alpha$  as a fitting parameter at angle  $30^\circ$  (Fig. 4).

We can see that our model is capable of describing accurately the experimental bidirectional reflectance of snow. It has no free parameters except the value of  $R$  at  $\vartheta = 30^\circ$ , in contrast with Hapke's model<sup>33</sup> as applied to snow. In particular, it is assumed in the framework of Hapke's model<sup>33,34</sup> that

$$R = \frac{\omega_0}{4(\xi + \eta)} \{[1 + s(g)]p(\theta) + H(\xi)H(\eta) - 1\}, \quad (15)$$

where  $\omega_0$  is the single-scattering albedo,  $p(\theta)$  is the phase function, and

$$s(g) = \frac{B_0}{1 + (1/h)\tan(g/2)}. \quad (16)$$

Here  $h$  and  $B_0$  are free parameters of the theory and  $g$  is the asymmetry parameter. Function  $H(\xi)$  can be calculated approximately with<sup>33</sup>

$$H(\xi) = \frac{1 + \xi}{1 + \xi\sqrt{1 - \omega_0}}. \quad (17)$$

For Fig. 4 we used the following values of parameters in Eqs. (15) and (16):  $B_0 = 1.0$ ,  $\omega_0 = h = 0.995$ , and the HG phase function  $p(\theta)$  with  $g = 0.449$ . Domingue *et al.*<sup>34</sup> found that this set of parameters gives best fits of the measurements derived from Hapke's model presented in Fig. 4.

It follows that both our snow model and that which was derived according to Hapke's theory explain the

almost constant value of the reflection function in a range of viewing angles smaller than 50° (near-nadir observations). This fact has also been confirmed by experiment.<sup>32</sup> However, our theory gives better agreement with measurements at the range of angles 45°–80°. Note that the use of a more-complex model of the phase function in Eq. (15) fails to improve the accuracy of Hapke's model to any great degree.<sup>34</sup>

Parameter  $\alpha$  obtained from fitting measurement data<sup>32</sup> by Eq. (1) and that calculated from values of  $g$  and  $\omega_0$  of Hapke's model  $\{\alpha = 4[(1 - \omega_0)/3(1 - g)]^{1/2}$  (Ref. 12) are similar. In particular, it is equal to 0.2 in the framework of our model and is only 10% larger (0.22) when it is derived from the fitting techniques based on Hapke's equation.

### 3. Local Optical Characteristics of Snow

#### A. Transport Path Length

Until now we have considered mostly the global optical characteristics of snow such as its bidirectional reflectance and albedo. Let us turn to the description of snow's local optical characteristics related to Eq. (1). In particular, we wish to establish the relation of parameters  $l_{\text{abs}}$  and  $l_{\text{tr}}$  to the microphysical characteristics of snow. This will also lead to the relationship between  $\alpha$  [Eq. (4)] and grain size  $d$ .

Let us start from  $l_{\text{tr}}$ . This parameter is defined by the following equation<sup>12</sup>:

$$l_{\text{tr}} = \frac{1}{\sigma_{\text{ext}}(1 - g)}, \quad (18)$$

where  $\sigma_{\text{ext}}$  is the extinction coefficient and  $g$  is the asymmetry parameter. For the large particles considered here,  $\sigma_{\text{ext}}$  and  $g$  are given as

$$\sigma_{\text{ext}} = (\langle C_{\text{ext}}^D \rangle + \langle C_{\text{ext}}^G \rangle)N, \quad (19)$$

$$g = \frac{\langle C_{\text{sca}}^D g^D \rangle + \langle C_{\text{sca}}^G g^G \rangle}{\langle C_{\text{sca}}^D \rangle + \langle C_{\text{sca}}^G \rangle}, \quad (20)$$

where  $N$  is the number of grains in a unit volume.  $G$  and  $D$  signify the contributions<sup>11,12</sup> of geometric optics ( $G$ ) and diffraction ( $D$ ) processes to extinction cross section  $C_{\text{ext}}$ , scattering cross section  $C_{\text{sca}}$ , and asymmetry parameter  $g$ . The angle brackets mean averages with respect to the geometrical characteristics of snow grains (size, shape, and orientation).

It follows from Eqs. (18)–(20) and the assumption that  $C_{\text{sca}} \approx C_{\text{ext}}$ , which is valid for the weakly absorbing media considered here, that

$$l_{\text{tr}} = \frac{1}{N(1 - \mathbb{Q}\langle g^G \rangle)\langle C_{\text{sca}}^G \rangle}, \quad (21)$$

where  $\mathbb{Q} = \langle C_{\text{sca}}^G g^G \rangle / \langle C_{\text{sca}}^G \rangle \langle g^G \rangle$ . Note that we have also used<sup>12</sup>  $g^D \approx 1$ .

Equation (21) shows that the transport path length in snow is defined by the geometrical part of the scattered field. This field is affected little by the close-packed effects (but is affected significantly by diffraction).<sup>10,12,33</sup> Therefore we can neglect consid-

eration of the close-packed effects in the calculation of  $l_{\text{tr}}$  because of their mutual cancellation. This is an important point.

It is known<sup>11,12</sup> that

$$\langle C_{\text{sca}}^G \rangle = \langle \Sigma \rangle / 4 \quad (22)$$

for nonspherical nonabsorbing convex particles in a random orientation, independently of refractive index  $m$  of grains and their exact shape. Here  $\langle \Sigma \rangle$  is the average surface area of particles.

It follows from Eqs. (21) and (22) that

$$l_{\text{tr}} = \frac{4}{N\langle \Sigma \rangle(1 - \langle g^G \rangle)}, \quad (23)$$

where we have assumed that  $\mathbb{Q} = 1$ . Such is exactly the case for nonabsorbing large spherical particles. Then  $g^G$  does not depend on the size of particles, and  $\langle C_{\text{sca}}^G g^G \rangle = \langle C_{\text{sca}}^G \rangle \langle g^G \rangle$ . We assume that this equality holds approximately for snow as a whole.

Equation (23) can be written in a slightly different form, introducing the volumetric concentration of snow grains,  $C_v$ :

$$C_v = N\langle V \rangle, \quad (24)$$

where  $\langle V \rangle$  is the average volume of grains. Then we have

$$l_{\text{tr}} = \frac{2d}{3(1 - \langle g^G \rangle)C_v}, \quad (25)$$

where

$$d = 6 \frac{\langle V \rangle}{\langle \Sigma \rangle}. \quad (26)$$

Equation (26) can be taken as a definition of effective grain size  $d$  for such a complex medium as snow. Note that for monodispersed spheres  $d$  is equal to their diameter. It follows for polydispersed media composed of spherical particles that  $d = 2a_{\text{ef}}$ , where  $a_{\text{ef}}$  is the effective radius, defined as the ratio of the third to the second moment of the particle size distribution.

The value of  $C_v$  is close to 1/3 for snow.<sup>2</sup> This means that  $l_{\text{tr}} \approx 2d/(1 - \langle g^G \rangle) \gg \lambda$  because  $d \gg \lambda$  and  $0 < g^G < 1$  and also points to the possibility of the application of the radiative transfer equation to the problems of snow optics.

It follows from Eq. (25) that the ratio  $M$  of transport lengths for media with spheres to that for media with nonspherical particles with the same values of  $C_v$  and  $d$  is given by the following formula:

$$M = \frac{1 - \langle g_n^G \rangle}{1 - \langle g_s^G \rangle}, \quad (27)$$

where  $s$  and  $n$  here and below denote spherical and nonspherical scattering, respectively. Note that  $g_n^G \approx 1/2$  for fractal particles considered here.<sup>35</sup> The value of the asymmetry parameter for large monodispersed spherical ice particles as a function of

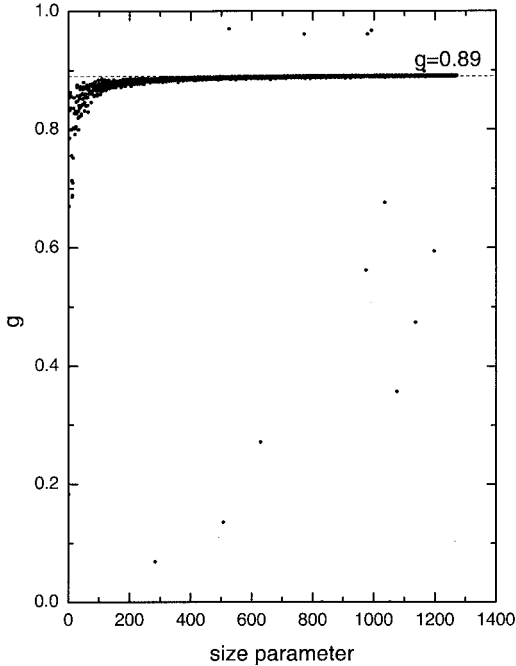


Fig. 5. Dependence of asymmetry parameter  $g$  on size parameter  $x$ , obtained from Mie theory for monodispersed spherical particles that have refractive index  $1.31 - 10^{-7}i$ .

size parameter  $x = \pi d/\lambda$  is presented in Fig. 5. We can see that  $g \approx 0.89$  for large ice spheres. This means that<sup>12</sup>  $g_s^G = 2g - 1 \approx 0.78$ , which gives, when Eq. (27) is taken into account,  $M = 2.27$ . Therefore the transport path length in the medium composed of fractal particles is approximately two times smaller than in a medium with spherical ice particles that has the same values of  $C_v$  and  $d$ . In particular, we have  $l_{\text{tr}}^s = 2.27 l_{\text{tr}}^n$ , which has important consequences for optical particle sizing in snow. We consider this issue in more detail in Section 4 below.

### B. Absorption Path Length

Let us study absorption path length  $l_{\text{abs}}$  now. It is defined as the inverse value of absorption coefficient  $\sigma_{\text{abs}}$ :  $l_{\text{abs}} = 1/\sigma_{\text{abs}}$ , where  $\sigma_{\text{abs}} = N\langle C_{\text{abs}} \rangle$  and  $\langle C_{\text{abs}} \rangle$  is the average absorption cross section per particle. In principle,  $\langle C_{\text{abs}} \rangle$  can also depend on the number of particles  $N$  for close-packed media such as snow fields.<sup>36,37</sup> However, *in situ* experiments<sup>38</sup> show that snow albedo [and therefore  $\alpha$ , see Eq. (9)] does not depend on  $N$ . The value of  $\alpha \sim \sqrt{l_{\text{abs}}/l_{\text{tr}}}$  is independent of  $N$  if  $\langle C_{\text{abs}} \rangle$  is not a function of  $N$ . Therefore we neglect the effects of close-packed media in the calculation of  $l_{\text{abs}}$  and write

$$l_{\text{abs}} = \frac{\langle V \rangle}{C_v \langle C_{\text{abs}} \rangle}, \quad (28)$$

where we have accounted for Eq. (24).

Let us derive an approximate expression for the value of  $C_{\text{abs}}$  for a particle of an arbitrary shape, as it

is needed in snow optics. For this we use the definition of  $C_{\text{abs}}$ <sup>12</sup>:

$$C_{\text{abs}} = \frac{k}{|\mathbf{E}_0|^2} \int_V \epsilon''(\mathbf{r}) \mathbf{E}(\mathbf{r}) \mathbf{E}^*(\mathbf{r}) d^3 r, \quad (29)$$

where  $k = 2\pi/\lambda$ ,  $\lambda$  is the wavelength,  $V$  is the volume of a particle,  $|\mathbf{E}_0|$  is the absolute value of incident electric field vector  $\mathbf{E}_0$ ,  $\epsilon'' = 2n\chi$  is the imaginary part of the relative dielectric permittivity of a particle,  $m = n - i\chi$  is the complex refractive index of a particle, and  $\mathbf{E}(\mathbf{r})$  is the value of the electric field inside a particle at the point with radius vector  $\mathbf{r}$ . We assume that

$$\mathbf{E}(\mathbf{r}) = \mathbf{E}_0 \sum_{s=0}^{\infty} a_s(\mathbf{r}) \exp[i\phi_s(\mathbf{r})], \quad (30)$$

which corresponds to the representation of  $\mathbf{E}(\mathbf{r})$  by a linear combination of simple waves with amplitudes  $a_s \mathbf{E}_0$  and phases  $\phi_s$ . It follows from Eq. (30) that

$$|\mathbf{E}|^2 = |\mathbf{E}_0|^2 \sum_{s=0}^{\infty} a_s^2 \exp(-2\phi_s''), \quad (31)$$

where  $\phi_s'' = \text{Im}(\phi_s)$  and we have neglected the phenomenon of interference, which is of no importance for snow grains with  $d \gg \lambda$ . Then, using the fact that  $\phi_s''$  is a small parameter for weakly absorbing grains, we obtain

$$|\mathbf{E}(\mathbf{r})|^2 = \beta(\mathbf{r}) |\mathbf{E}_0|^2, \quad (32)$$

where  $\beta(\mathbf{r}) = \sum_{s=0}^{\infty} a_s^2(\mathbf{r})$ .

It follows from Eqs. (29) and (32) that

$$C_{\text{abs}} = k \beta(\mathbf{r}_0) \int_V \epsilon''(\mathbf{r}) d^3 r, \quad (33)$$

where we have used the equality

$$\int_V \psi(\mathbf{r}) F(\mathbf{r}) d\mathbf{r} = \psi(\mathbf{r}_0) \int_V F(\mathbf{r}) d\mathbf{r}. \quad (34)$$

The value of  $\mathbf{r}_0$  is generally not known.

We neglect the internal inhomogeneity of grains. Then it follows from Eq. (33) that

$$C_{\text{abs}} = n \beta \gamma V, \quad (35)$$

where  $\gamma = 4\pi\chi(\lambda)/\lambda$  is the absorption coefficient of ice. Also, we have

$$\langle C_{\text{abs}} \rangle = B \gamma \langle V \rangle, \quad (36)$$

where  $B = n\langle \beta \rangle$  and we have assumed that  $\langle \beta V \rangle \approx \langle \beta \rangle \langle V \rangle$ . One can obtain from Eqs. (28) and (36)

$$l_{\text{abs}} = \frac{1}{B \gamma C_v}. \quad (37)$$

Let us check the applicability of Eq. (35) for a specific case of spherical particles. To do this we calculated the ratio  $B = C_{\text{abs}}/\gamma V$  with Mie theory for

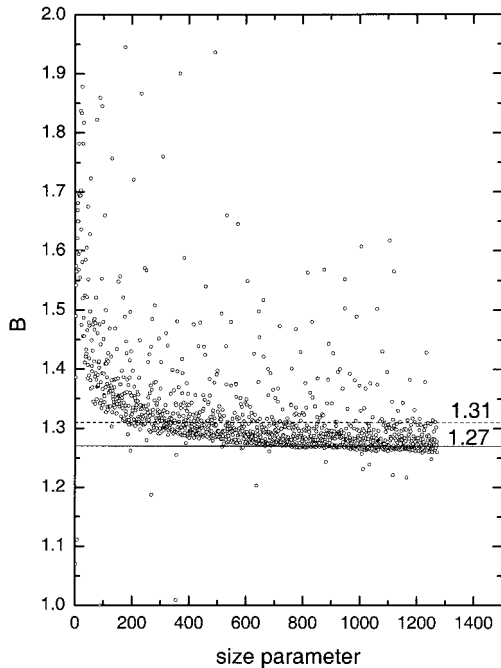


Fig. 6. Dependence of absorption enhancement parameter  $B$  on size parameter  $x$  obtained from Mie theory for monodispersed spherical particles that have refractive index  $1.31 - 10^{-7}i$ .

monodispersed spheres with refractive index  $m = 1.31 - 10^{-7}i$  at  $\lambda = 0.55 \mu\text{m}$  as a function of size parameter  $x = \pi d/\lambda$ . The results are given in Fig. 6. We see that indeed  $B$  depends only weakly on  $x$  if we neglect the effects of interference, which are of no importance for snow optics because of the nonspherical shape of grains and their polydispersity. The numerical data for the value of  $B$  scatter from 1.27 to 1.31 for cases relevant to snow optics problems ( $x = 500-1200$ ). This gives a variability of less than 3%. We take the value  $B \approx 1.27$  for estimations in this paper, which is similar to that used by Bohren<sup>39</sup> ( $B \approx 1.26$ ). This means [Eq. (32)] that  $\beta = B/n \approx 1.0$  (with errors smaller than 3%) for ice spheres in the visible, where  $n \approx 1.31$ . Also, we have on physical grounds  $\beta \rightarrow 1$  as  $n \rightarrow 1$  [or  $C_{\text{abs}} \rightarrow \gamma V$  (Ref. 12)]. This means that  $\beta$  is highly robust against variations in the refractive index for the range of  $n$  relevant to snow optics problems.

The values of  $B$  for spheroids and hexagonal cylinders with various aspect ratios were tabulated in Refs. 12 and 40. In particular, it was found that  $B = 1.2-2.1$  for spheroids and  $B = 2.2-2.5$  for hexagonal cylinders if it was assumed that the ratio of their axes is in the range 0.5–2.0. The average of  $B$  for the interval 1.2–2.5 is 1.85, which is close to our estimation of  $B \approx 1.84$  for fractal particles obtained from geometrical optics Monte Carlo calculations. The details of the code that we used to find  $B$  for fractals are given elsewhere.<sup>28</sup> The close correspondence of  $B$  for fractals and a mixture of particles that have various shapes is not surprising when one takes into account the fact that chaotic scattering and absorption by media with particles of diverse shapes should

approach those of a single, extremely irregular particle such as a fractal.

Therefore we propose to use the value  $B = 1.84$  in snow optics instead of  $B = 1.27$  as for spheres. This proposal, however, should be checked against carefully planned experiments for natural snow. We note that the value of  $B$  may also depend on the age of the snow and on temperature.

Our estimations and those given in Refs. 12 and 40 allow us to conclude that large, weakly absorbing nonspherical ice particles generally have larger absorption cross sections than spheres of the same volume ( $B_n > B_s$ ). This means also that  $l_{\text{abs}}^s > l_{\text{abs}}^n$ .

In particular, we have for ice particles  $l_{\text{abs}}^s \approx 1.45l_{\text{abs}}^n$  if the volume concentration of snow grains is fixed. Recall that  $l_{\text{tr}}^s = 2.27l_{\text{tr}}^n$ . This means that the ratio  $l_{\text{tr}}/l_{\text{abs}}$ , which is of importance for reflectance problems [Eqs. (1) and (4)] is 1.57 times larger for spheres than for fractal particles with the same values of the product  $\gamma d$ .

As can be seen from Eqs. (1) and (4), this ratio can easily be determined from reflectance measurements. It is proportional to the size of the grains [Eqs. (25) and (37)]:

$$\frac{l_{\text{tr}}}{l_{\text{abs}}} = \frac{2B\gamma d}{3(1 - \langle g^G \rangle)}. \quad (38)$$

In particular, we have  $l_{\text{tr}}/l_{\text{abs}} \approx 2.45\gamma d$  for fractal particles and  $l_{\text{tr}}/l_{\text{abs}} \approx 3.85\gamma d$  for spheres. It follows from Eq. (38) that  $d = \mathcal{I}l_{\text{tr}}/\gamma l_{\text{abs}}$ , where  $\mathcal{I} = 3(1 - \langle g^G \rangle)/2B$ . Let us suppose that the ratio  $l_{\text{tr}}/\gamma l_{\text{abs}}$  is exactly known (the ratio  $l_{\text{tr}}/l_{\text{abs}}$  is determined from the snow's reflectance when the absorption coefficient of ice,  $\gamma$ , is known with a high degree of accuracy). Then the error of the grain-size estimation that is due to the spherical shape assumption is given by  $\delta = 1 - \mathcal{I}_s/\mathcal{I}_n$ . Taking into account that  $\mathcal{I}_s \approx 0.26$  and  $\mathcal{I}_n \approx 0.408$ , we obtain that  $\delta \approx 0.4$ , which allows us to conclude that the uncertainty in the determination of the grain size that is caused by shape effects could reach 40%. Therefore retrievals of snow grain size based on Mie theory may greatly underestimate the value of  $d$ . This finding is a major result of our study. Note that *in situ* measurements also confirm that an optically equivalent (in terms of spectral albedo fitting) diameter of the snow grain size is smaller than that measured *in situ*. This problem has been addressed, e.g., by Aoki *et al.*,<sup>5</sup> who suggested that the spherical approximation gives not the value of  $d$  defined in Eq. (26) but rather a dimension of a narrower portion of broken crystals or the branch width of dendrites.

The value of  $\alpha \sim \sqrt{l_{\text{tr}}/l_{\text{abs}}}$  is approximately 1.25 times larger for spheres than for fractals. We conclude, therefore, that although values of  $l_{\text{abs}}$  and  $l_{\text{tr}}$  differ considerably for spheres compared with fractals (see above), the difference is more moderate for the value of  $\alpha$ , which determines the albedo of snow. Nevertheless, we stress that the use of the Mie model for the calculation of  $\alpha$  with Eq. (4) leads to an overestimation of  $\alpha$  by 25% compared with the fractal

model. This leads to an overestimation of the snow's heating (larger  $\alpha$ ) if the spherical-particle model is used and also gives the same error in the value of  $1 - r$  as in  $r \rightarrow 1$  [Eq. (6)].

#### 4. Determination of Snow Grain Size by Reflectance Spectroscopy

Equations (2), (4), (8), (25), and (37) can be used for rapid yet accurate estimations of the spectral reflectance of snow for various observation geometries and snow grain sizes. These estimates can be used for several applications, including retrieval of the properties of aerosols and clouds over snow fields.

However, the most promising area for application of our semianalytical theory is in the determination of snow grain size by use of data from airborne and satellite-based radiometers and spectrometers.

Snow grain size is an important parameter, which can be used, in particular, as an indicator of the age of snow. Changes in grain size help to identify snow dunes, melt areas, and regions of blue ice. They often indicate changes in the snowpack's energy balance.

The rate of grain growth is exponentially proportional to temperature. This means that changes in grain size are indicators of thermodynamic processes in the snowpack. The estimation of grain size is of importance for calculating the absorption of radiation in snowpack. Note that increased absorption of solar light by snow leads to increased probabilities of melting snow and avalanches.

To start with, let us find the analytical relationship between the snow's bidirectional reflectance and the snow's grain size. For this we substitute Eqs. (4), (25), and (37) into Eq. (1):

$$R = R_0 \exp(-bf\sqrt{\gamma d}), \quad (39)$$

where

$$b = \frac{4}{3} \left[ \frac{2B}{(1 - \langle g^G \rangle)} \right]^{1/2}. \quad (40)$$

We conclude from Eq. (39) that the spectral dependence of  $\ln R$  can be presented as a linear function of  $X(\lambda) = \sqrt{\gamma(\lambda)}$ . In particular, it follows that  $\ln R(\lambda) = s + vX(\lambda)$ , where  $s = \ln R_0$  and  $v = -bf\sqrt{d}$ . Our estimations show that the spectral variability of parameters  $s$  and  $v$  can be neglected.

Note that it follows [see Eqs. (1) and (39)] that

$$\alpha = b\sqrt{\gamma d}. \quad (41)$$

This means that the spectral reflectance of snow is determined by the absorption of light on the length equal to grain diameter  $d$  (e.g., by the parameter  $c = \gamma d$ ). This is similar in some respects to the conventional transmittance spectroscopy. Then the value of  $c$  is directly measured and  $\gamma$  is obtained as the ratio  $c/d$ , where  $d$  is the length of the measured cell.

Substituting the values  $B \approx 1.84$  and  $\langle g^G \rangle \approx 0.5$  into Eq. (40), we obtain for media with fractal particles  $b_n \approx 3.62$ . It follows that, for spheres with  $B \approx$

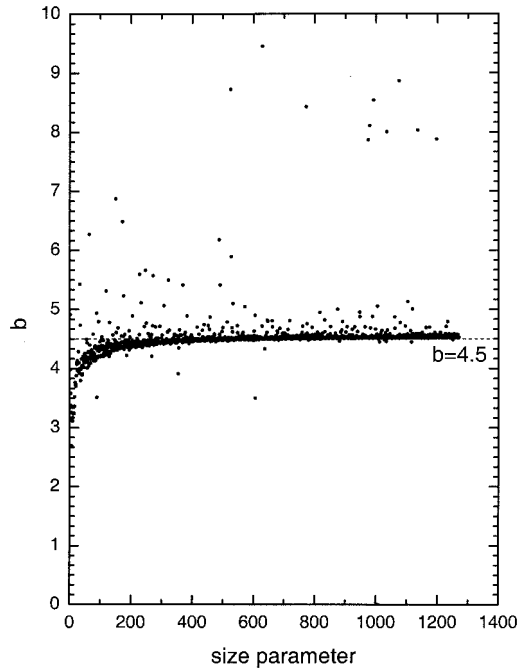


Fig. 7. Same as in Fig. 6, except for the value of  $b$ .

1.27 and  $\langle g^G \rangle \approx 0.78$ ,  $b_s \approx 4.53$ . Figure 7 confirms this finding for spheres. We have, therefore,  $b_s/b_n \approx 1.25$ , the result that has already been quoted above. Therefore we conclude that the value of  $b$  for spheres is approximately 25% too high than that of fractal particles. Therefore smaller grains are needed to produce the same value of  $R$  [Eq. (39)] for snow made from ice spheres as for fractal snow.

It follows from Eq. (39) that

$$d = \frac{1}{\gamma b^2 f^2} \ln^2 \left( \frac{R}{R_0} \right). \quad (42)$$

This physically based equation can be used as an alternative to techniques for retrieval of snow grain size based on fitting procedures (see, e.g., Ref. 6). Equation (42) can also be used for estimates of the influence of various factors on the retrieved value of  $d$ . In particular, we obtain from Eq. (42) that the uncertainty  $\delta$  in the value of  $\gamma$  translates into the same value of uncertainty in the value of  $d$ .

It follows from Eq. (42) under the assumption that  $R_0 \approx 1.0$  (Fig. 2) for both spheres and fractals that  $d_n/d_s = (b_s/b_n)^2 \approx 1.6$ . Therefore we have  $d_n \approx 1.6d_s$ , and currently used remote-sensing techniques may substantially underestimate the sizes of snow grains. Also, we have  $\delta = 1 - d_s/d_n \approx 0.4$ , as was outlined above. Note that the necessity to account for atmospheric scattering above snow (see, e.g., Ref. 5) complicates the estimation of  $\delta$  given above.

It should be emphasized that all parameters in Eq. (42) (except  $R_0$ ) are given by simple analytical formulas specified above. This allows for the determination of  $d$  from the measured value of  $R$  if  $R_0$  is obtained from precalculated lookup tables for fractal particles. Note that  $R_0$  is close to 1 for fractal par-

ticles at nadir observation (Fig. 2) and nongrazing solar angles. Approximate equations for  $R_0$  can be found elsewhere.<sup>12,15,22</sup>

The information on  $R_0$  is not needed if the plane albedo of snow is measured. Then we have [Eq. (9)]

$$d = \frac{C \ln^2(r_p)}{\gamma(1 + 2 \cos \vartheta_0)^2}, \quad (43)$$

where  $C = 49/9b^2 \approx 0.42$  and we have accounted for the fact that  $b \approx 3.6$  for fractals. This allows for the immediate determination of  $d$  from  $r_p$  if solar zenith angle  $\vartheta_0$  is known. It follows from Eq. (43) that uncertainty  $\delta$  in the value of  $\gamma$  leads to the same value of uncertainty in the retrieved grain size  $d$ , as was already shown above.

An even simpler equation can be derived for  $d$  if spherical albedo  $r$  of snow is measured. Indeed, it follows from Eq. (A8) of Appendix A in combination with Eq. (41) that

$$r = \exp(-b \sqrt{\gamma d}) \quad (44)$$

and, therefore, that

$$d = \frac{1}{\gamma b^2} \ln^2 r. \quad (45)$$

Interestingly, Eq. (44) is transformed into the well-known formula<sup>39,41</sup>

$$r = 1 - b \sqrt{\gamma d} \quad (46)$$

for small values of light absorption in snow. Note that Bohren<sup>39</sup> proposed the value  $b = 6.0$ , which is somewhat larger than the corresponding value for fractal particles (see above). It is also larger than values of  $b$  for asymptotically large ice spheres (Fig. 7). Clearly, only experiments can determine the possible range of change of this parameter in natural snow. Note that we have from Eq. (46) that  $b = (1 - r)/\sqrt{\gamma d}$  for weakly absorbing media. This allows us to find the value of  $b$  from experimental measurements.

The accuracy of Eq. (44) is studied in Fig. 8 by use of experimental data for snow reflectance obtained in Antarctica,<sup>42</sup> where snow pollution is of only minor importance. The data for refractive indices of ice were taken from Ref. 43. There is a problem with the choice of an appropriate value of  $d$  that is representative for measurements. Note that Grenfell *et al.*<sup>42</sup> give vertical profiles of grain size measured visually in the field at the South Pole (1985–1986) and the Vostok, Antarctica (1990–1991) stations. The average values of  $d$  were 0.15 mm for the South Pole station and 0.22 mm for the Vostok station (in the upper 10 cm of snow; see Table 3 of Ref. 42). They also determined average snow size profiles at the South Pole station (1986), obtained by the analysis of photographs ( $d = 0.28$  mm in the upper 10 cm of snow), as presented in Table 4 of Ref. 42. The resultant average grain diameter was 0.22 mm, so we used this diameter in our calculations for Fig. 8.

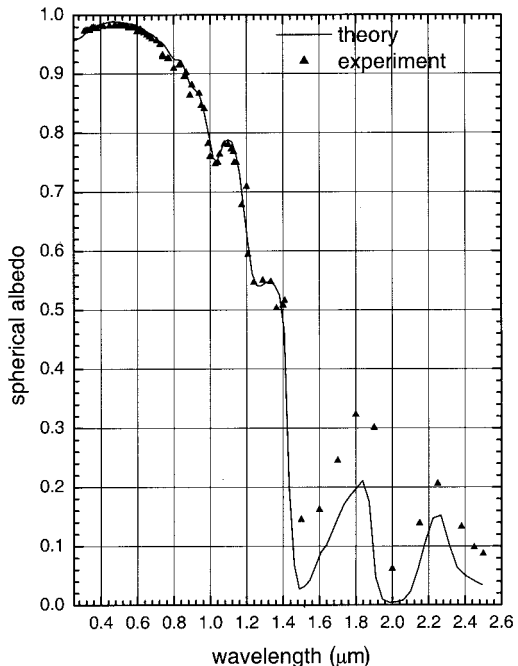


Fig. 8. Dependence of spherical albedo on wavelength according to measurements<sup>42</sup> and calculations made with Eq. (44) at  $b = 3.6$  and  $d = 0.22$  mm. The data for refractive indices of ice are taken from Ref. 43.

It follows from Fig. 8 that experimental data can be explained by the theory developed here for a wide spectral range starting from the UV until approximately 1.4  $\mu\text{m}$ . For larger wavelengths the assumption of weakly absorbing media used extensively in this paper is not valid, so errors are increased. Then the exact radiative transfer equation with numerical calculations of the local optical characteristics of snow's fractal grains should preferably be used. Such numerical results for a semi-infinite homogeneous snow layer have already been reported.<sup>9</sup> The simplicity of the retrieval scheme as emphasized above is lost then, however.

Clearly, such good fits as in Fig. 8 at  $\lambda \leq 1.4 \mu\text{m}$  (and also for larger wavelengths) can be obtained with Mie theory as well. However, then the value of  $d$  is merely a fitting parameter. This parameter can differ substantially from the snow grain size defined by Eq. (26), as was emphasized above. This finding underlines the necessity of careful analysis of the spectral reflectance of snow relative to determination of the snow's grain size.

The analytical solution of the inverse problem proposed here can be applied to uniform snow only. Aged snow is characterized by the vertical inhomogeneity of its physical properties, however. This means that the value of  $d$  derived from Eq. (42) will change with wavelength for vertically inhomogeneous snow. This change can be advantageous, however. Indeed, in this case the reflection function is influenced by different parts of the layer, depending on the wavelengths. Clearly, highly absorbing wavelengths will give information on the microstruc-

ture of the top snow layer only. Deeper layers of snow can be sensed by weakly absorbing wavelengths. This peculiarity was first studied by Li *et al.*, who used data from the Airborne Visible/Infrared Imaging Spectrometer at wavelengths of 0.86, 1.05, 1.24, and 1.73  $\mu\text{m}$ . Clearly, this issue deserves further exploration. For this exploration, however, our technique should be extended to vertically inhomogeneous media as could be done, e.g., by use of Chamberlain's effective-reflective-layer technique.<sup>21,44</sup>

Another important issue that can be addressed in the framework of our approach is the identification of snow pollution (e.g., by soot). Then, assuming that the diameters of grains are obtained from IR channels (see, e.g., Ref. 45), where  $\gamma$  is determined almost exclusively by ice absorption, it follows from Eq. (42) that, in the visible, where ice is almost transparent,

$$\gamma = \frac{1}{b^2 f^2 d} \ln^2 \left( \frac{R}{R_0} \right). \quad (47)$$

The value of  $\gamma$  can deviate substantially from zero because of snow pollution. Clearly, the derived value of  $\gamma$  can be used for estimation of the concentration of pollutants.<sup>45</sup> Then the information on the type of pollutant (e.g., snow, dust, or both) should be known *a priori* or assessed from spectral curves  $R(\lambda)$  [and related spectra  $\gamma(\lambda)$ ].

Equation (47) offers a simple way to estimate the relative absorption coefficient of ice in snow  $\gamma_r(\lambda) = \gamma(\lambda)/\gamma(\lambda_0)$ , where  $\lambda_0$  is the selected reference wavelength. That is, it follows from Eq. (47) that

$$\gamma_r(\lambda) = \frac{\ln^2[\Xi R(\lambda)]}{\ln^2[\Xi R(\lambda_0)]}, \quad (48)$$

where we have accounted for the fact that  $\Xi = 1/R_0(\lambda_0)$  does not vary considerably with wavelength.

An even simpler result follows from Eqs. (43) and (45):

$$\gamma_r(\lambda) = \frac{\ln^2 r_p(\lambda)}{\ln^2 r_p(\lambda_0)} = \frac{\ln^2 r(\lambda)}{\ln^2 r(\lambda_0)}. \quad (49)$$

This allows for the direct determination of the relative ice absorption coefficient from measurements of spectral albedo.

## 5. Conclusions

The science of snow optics is still in its infancy. Simplified models based on sparsely distributed ideal spherical particles are used studying the optical properties of snow and also for deriving characteristics of snow by use of data from airborne and spaceborne spectrometers and radiometers.<sup>46–48</sup> Such models are remote from reality. Snow is an extremely complex medium composed of nonspherical, irregularly shaped grains in contact with one another. This influences the radiative and polarization characteristics of snow considerably. Nevertheless, it was found in previous studies<sup>3–5</sup> that the spherical-particle model fits the measured spectral albedo re-

flectance spectra of snow quite well. In this paper we have clarified the physics behind this result and shown that it cannot be considered a proof of the spherical model without independent control of the snow grain's size. Also, the spherical approximation fails to explain the behavior of the snow's bidirectional reflectance.<sup>5,32,34</sup> We draw the reader's attention to the fact that, unlike most conventional approaches, which compute the reflectance of snow with radiative transfer codes, this paper offers the use of an exponential asymptotic analytical equation for the reflectance of snow. This simple solution is shown to be highly accurate in the case studied.

The main objective of this paper is to introduce and discuss a new approach to snow optics with a more-realistic model of snow as a medium with nonspherical and close-packed snow grains. However, the results obtained can also be used far beyond the rather narrow topic considered here. In particular, they can be applied to other weakly absorbing light-scattering media with a complex structures, including whitecaps and bright soils. The last issue of particular importance for planetary spectroscopy.<sup>33</sup>

We propose to use a fractal-particle model instead of the spherical-particle model usually applied in snow optics. Clearly the fractal-particle model of snow is closer to reality than the spherical-grain assumption. We emphasize that the use of this more-sophisticated model does not lead to any complications (at least, in the UV, visible, and a considerable portion of the near-IR spectral regions, where absorption of light by snow is weak). The difference between these two models lies in the final equation for snow's reflectance as different values of a form factor [ $b$  in Eq. (42)], which account for the shape effects. The value of this form factor could serve as a criterion with which to estimate and choose the appropriate snow model; it could and should be controlled in special experiments with natural snow.

The use of the fractal model instead of the spherical model leads to  $\sim 40\%$  larger values of the retrieved snow grain size compared with output from the spherical model. This means that retrieval techniques based on Mie theory will bias grain size [defined by Eq. (26)] considerably. This fact was underlined long ago by Grenfell *et al.*,<sup>49</sup> who found disagreement (by 50%, which is close to our estimation) between measured and retrieved (in the framework of the spherical approximation) values of  $d$ . Similar results were reported in Refs. 5, 50, and 51. We believe that we have managed to establish the physics behind these findings.

Note that the comparison of remotely sensed snow grain sizes with those determined *in situ* made in Refs. 46–48 also showed that remote-sensing techniques for measuring snow based on the spherical approximation do underestimate snow grain characteristics. It was argued that this underestimation could be due to snow pollution or to subpixel scene heterogeneity<sup>48</sup> (e.g., unaccounted for contributions from thin snow layers, vegetation, soil, and rock).

However, the nonspherical shapes of snow crystals can also contribute to the discrepancy found.

To avoid the influence of pollution (e.g., by soot) and atmospheric molecular absorption, one should measure snow reflectance in the near-IR spectral range outside gaseous absorption bands. Measuring in this range also minimizes the contribution of atmospheric scattering. Then one can use the obtained value of the snow grain size to find the level of light absorption in visible. The difference between this value and that of the absorption of pure snow gives the strength of snow pollution.<sup>45</sup> Similar techniques can be used to identify various life forms in snow (see, e.g., Ref. 52). This could be of importance in the analysis of data from satellites orbiting other planets including Mars. Note that the unconfirmed possibility of life forms outside our terrestrial environment is a subject of intensive research.<sup>53,54</sup>

The analytical equations that we obtained can be applied for the solution of the inverse problem of the snow grain determination by space-based, airborne, and ground measurements. They can be also used to improve the snow hydrology for global circulation models.<sup>55</sup>

For the sake of simplicity, only horizontally homogeneous snow layers of an infinite depth have been considered in this paper. The extension of this approach to finite and to vertically inhomogeneous snow layers can easily be made by use of an approach similar to that described above (see, e.g., Refs. 12, 15, and 21). Remote sensing of heterogeneous snow fields (e.g., with soil and vegetation included in the scene studied) and issues related to the determination of snow cover can be explored by use of a combination of our approach with the linear or nonlinear multiple-end-member spectral mixtures analysis proposed in Ref. 48.

#### Appendix A. Plane Albedo

Here we derive a simple analytical equation for the plane albedo of a semi-infinite snow layer. The value of  $r_p$  is defined by the following integral:

$$r_p = \frac{1}{\pi} \int_0^{2\pi} d\varphi \int_0^1 \eta d\eta R(\xi, \eta, \varphi), \quad (\text{A1})$$

where  $R(\xi, \eta, \varphi)$  is the bidirectional reflectance,  $\xi$  and  $\eta$  are cosines of the incident and viewing zenith angles, respectively, and  $\varphi$  is the azimuthal angle. Let us substitute Eq. (1) into Eq. (A1). Then it follows that

$$\begin{aligned} r_p &= \frac{1}{\pi} \int_0^{2\pi} d\varphi \int_0^1 \eta d\eta R_0(\xi, \eta, \varphi) \\ &\times \exp \left[ -\alpha \frac{K_0(\xi) K_0(\eta)}{R_0(\xi, \eta, \varphi)} \right]. \end{aligned} \quad (\text{A2})$$

The value of  $r_p$  can be found from Eq. (A2) only by use of numerical integration.

Let us obtain an approximate analytical result for the plane albedo, using the expansion

$$\exp \left[ -\alpha \frac{K_0(\xi) K_0(\eta)}{R_0(\xi, \eta, \varphi)} \right] = \sum_{s=0}^{\infty} \frac{(-1)^s K_0^s(\xi) K_0^s(\eta)}{s! R_0^s(\xi, \eta, \varphi)}. \quad (\text{A3})$$

Then it follows from Eqs. (A2) and (A3) that

$$r_p = 1 - \alpha K_0(\xi), \quad (\text{A4})$$

where we have neglected nonlinear terms in Eq. (A3) and accounted for the identities<sup>16,20</sup>

$$\frac{1}{\pi} \int_0^{2\pi} d\varphi \int_0^1 \eta d\eta R_0(\xi, \eta, \varphi) = 1,$$

$$2 \int_0^1 K_0(\eta) \eta d\eta = 1. \quad (\text{A5})$$

Unfortunately, our derivation cannot be extended to nonlinear terms in Eq. (A3). Therefore we assume that  $r_p$  is governed by a similar law, as specified by Eq. (1):

$$r_p = \exp[-\alpha K_0(\xi)]. \quad (\text{A6})$$

This formula is transformed into Eq. (A4) for small values of  $\alpha$ .

Equation (A6) can be used to find the spherical albedo, defined as [Eq. (7)]

$$r = 2 \int_0^1 r_p(\xi) \xi d\xi. \quad (\text{A7})$$

Using Eq. (A6) and the same chain of arguments as above, we obtain from Eq. (A7)

$$r = \exp(-\alpha). \quad (\text{A8})$$

The accuracy of the derived equations was studied in Refs. 12, 15, 17, and 18.

The authors are grateful to A. Macke and M. I. Mishchenko for providing the computer codes used in this paper. We thank T. Nousiainen for calculation of the phase function of a Gaussian ice particle shown in Fig. 3. Substantial discussions with T. Aoki, I. L. Katsev, J. Lenoble, T. Nakajima, I. N. Polonsky, and A. S. Prikhach are very much appreciated.

This study was supported in part by the German Space Agency (grant 50EE0027) and the National Space Development Agency of Japan (grant G-0054).

#### References

1. A. W. Nolin and S. Liang, "Progress in bi-directional reflectance modeling and applications for surface particulate media: snow and soils," *Remote Sens. Rev.* **18**, 307–342 (2000).
2. R. A. Massom, H. Eicken, C. Haas, M. O. Jeffris, M. R. Drinkwater, M. Sturm, A. P. Worby, X. Wu, V. I. Lytle, S. Ushio, K. Morris, P. A. Reid, S. G. Warren, and I. Allison, "Snow on Antarctic ice," *Rev. Geophys.* **39**, 413–445 (2001).
3. S. G. Warren, "Optical properties of snow," *Rev. Geophys. Space Phys.* **2**, 67–89 (1982).
4. W. J. Wiscombe and S. G. Warren, "A model for the spectral

albedo of snow. I. Pure snow," *J. Geophys. Res.* **37**, 2712–2733 (1981).

5. T. Aoki, T. Aoki, M. Fukabori, A. Hachikubo, Y. Tachibana, and F. Nishio, "Effects of snow physical parameters on spectral albedo and bi-directional reflectance of snow surface," *J. Geophys. Res.* **105**, 10,219–10,236 (2000).
6. W. Li, K. Stamnes, and B. Chen, "Snow grain size retrieved from near-infrared radiances at multiple wavelengths," *Geophys. Res. Lett.* **28**, 1699–1702 (2001).
7. M. I. Mishchenko, L. D. Travis, and A. A. Lacis, *Absorption, Scattering, and Emission of Light by Small Particles* (Cambridge U. Press, Cambridge, 2002).
8. A. A. Kokhanovsky, *Polarization Optics of Random Media* (Springer-Praxis, Chichester, U.K., 2003).
9. M. I. Mishchenko, J. M. Dlugach, E. G. Yanovitskij, and N. T. Zakhrova, "Bidirectional reflectance of flat, optically thick particulate layers: an efficient radiative transfer solution and applications to snow and soil surfaces," *J. Quant. Spectrosc. Radiat. Transfer* **63**, 409–432 (1999).
10. A. P. Ivanov, V. A. Loiko, and V. P. Dik, *Light Propagation in Close-Packed Media* (Nauka i Tekhnika, Minsk, Belarus, 1988).
11. H. C. van de Hulst, *Light Scattering by Small Particles* (Dover, New York, 1981).
12. A. A. Kokhanovsky, *Light Scattering Media Optics: Problems and Solutions* (Springer-Praxis, Chichester, U.K., 2001).
13. L. Tsang, J. A. Kong, and R. T. Shin, *Theory of Microwave Remote Sensing* (Wiley-Interscience, New York, 1985).
14. G. V. Rozenberg, "Optical characteristics of thick weakly absorbing scattering layers," *Dokl. Akad. Nauk SSSR* **145**, 775–777 (1962).
15. E. P. Zege, A. P. Ivanov, and I. L. Katsev, *Image Transfer through a Scattering Medium* (Springer-Verlag, New York, 1991).
16. H. C. van de Hulst, *Multiple Light Scattering: Tables, Formulas and Applications* (Academic, New York, 1980).
17. A. A. Kokhanovsky, "Reflection and polarization of light by semi-infinite turbid media: simple approximations," *J. Colloid Interface Sci.* **251**, 429–431 (2002).
18. A. A. Kokhanovsky, "The accuracy of selected approximations for the reflection function of a semi-infinite turbid medium," *J. Appl. Phys. D* **35**, 1057–1062 (2002).
19. A. A. Kokhanovsky, V. V. Rozanov, E. P. Zege, H. Bovensmann, and J. P. Burrows, "A semi-analytical cloud retrieval algorithm using backscattering radiation in 04.–2.4  $\mu\text{m}$  spectral range," *J. Geophys. Res. D* **108**, 10.1029/2001JD001543 (2003).
20. I. N. Minin, *Radiative Transfer Theory in Planetary Atmospheres* (Nauka, Moscow, 1988).
21. E. G. Yanovitskij, *Light Scattering in Inhomogeneous Atmospheres* (Springer-Verlag, New York, 1997).
22. V. V. Sobolev, *Light Scattering in Planetary Atmospheres* (Nauka, Moscow, 1972).
23. R. C. Hubley, "Measurement of diurnal variations in snow albedo on Lemon Greek Glacier, Alaska," *J. Glaciol.* **2**, 560–563 (1955).
24. N. P. Rusin, *Meteorological and Radiative Regime of Antarctica* (Gidrometeoizdat, Leningrad, 1961).
25. B. Barkey, M. Bailey, K.-N. Liou, and J. Hallett, "Light-scattering properties of plate and column ice crystals generated in a laboratory cold chamber," *Appl. Opt.* **41**, 5792–5796 (2002).
26. K. Muinonen, T. Nusiaainen, P. Fast, K. Lumme, and J. I. Peltoniemi, "Light scattering by Gaussian random particles: ray optics approximation," *J. Quant. Spectrosc. Radiat. Transfer* **55**, 577–601 (1996).
27. T. Nusiaainen and K. Muinonen, "Light scattering by Gaussian, randomly oscillating raindrops," *J. Quant. Spectrosc. Radiat. Transfer* **63**, 643–666 (1999).
28. A. Macke, "Modellierung der Optischen Eigenschaften von Cirruswolken," Ph.D. dissertation, (University of Hamburg, Hamburg, Germany, 1994).
29. A. Macke, J. Mueller, and E. Raschke, "Scattering properties of atmospheric ice crystals," *J. Atmos. Sci.* **53**, 2813–2825 (1996).
30. P. Yang and K. N. Liou, "Single-scattering properties of complex ice crystals in terrestrial atmosphere," *Contrib. Atmos. Phys.* **71**, 223–248 (1998).
31. K. N. Liou, *Introduction to Atmospheric Radiation* (Academic, New York, 2002).
32. W. E. K. Middleton and A. G. Mungall, "The luminous directional reflectance of snow," *J. Opt. Soc. Am.* **42**, 572–579 (1952).
33. B. Hapke, *Theory of Reflectance and Emittance Spectroscopy* (Cambridge U. Press, Cambridge, 1993).
34. D. Domingue, B. Hartmon, and A. Verbiscer, "The scattering properties of natural terrestrial snow versus icy satellite surfaces," *Icarus* **128**, 28–48 (1997).
35. A. A. Kokhanovsky, "Optical properties of irregularly shaped particles," *J. Appl. Phys. D* **36**, 915–923 (2003).
36. A. P. Ivanov, S. A. Makarevich, and A. Y. Khairullina, "On specific features of radiation propagation in tissues and bioliquids with closely packed particles," *J. Appl. Spectrosc.* **47**, 662–668 (1987).
37. V. A. Loiko and G. I. Ruban, "Absorption and scattering of light by a photolayer with closely packed particles," *Opt. Spectrosc.* **88**, 834–839 (2000).
38. C. F. Bohren and R. L. Beschta, "Snowpack albedo and snow density," *Cold Regions Sci. Technol.* **1**, 47–50 (1979).
39. C. F. Bohren, "Colors of snow, frozen waterfalls, and icebergs," *J. Opt. Soc. Am.* **12**, 1646–1651 (1983).
40. A. A. Kokhanovsky and A. Macke, "Integral light scattering and absorption characteristics of large nonspherical particles," *Appl. Opt.* **36**, 8785–8790 (1997).
41. C. F. Bohren and B. R. Barkstrom, "Theory of the optical properties of snow," *J. Geophys. Res.* **79**, 4527–4535 (1974).
42. T. C. Grenfell, S. G. Warren, and P. C. Mullen, "Reflection of solar radiation by the Antarctic snow surface at ultraviolet, visible, and near-infrared wavelengths," *J. Geophys. Res.* **99**, 18,669–18,684 (1994).
43. S. G. Warren, "Optical properties of ice from the ultraviolet to the microwave," *Appl. Opt.* **23**, 1206–1225 (1984).
44. A. A. Kokhanovsky and V. V. Rozanov, "The physical parameterization of the top-of-atmosphere reflectron function for a cloudy atmosphere-underlying surface system: the oxygen A-band case study," *J. Quant. Spectrosc. Radiat. Transfer* (to be published).
45. E. P. Zege, A. A. Kokhanovsky, I. L. Katsev, I. N. Polonsky, and A. S. Prikhach, "The retrieval of the effective radius of snow grains and control of snow pollution with GLI data," in *Proceedings of Conference on Light Scattering by Nonspherical Particles: Theory, Measurements, and Applications*, M. I. Mishchenko, L. D. Travis, and J. W. Hovenier, eds. (American Meteorological Society, Boston, Mass., 1998), pp. 288–290.
46. M. Fily, B. Bourdilles, J. P. Dedieu, and C. Sergent, "Comparison of *in situ* and Landsat Thematic Mapper derived snow grain characteristics in the Alps," *Remote Sens. Environ.* **59**, 452–460 (1997).
47. A. W. Nolin and J. Dozier, "A hyperspectral method for remotely sensing the grain size of snow," *Remote Sens. Environ.* **74**, 207–216 (2000).
48. T. H. Painter, J. Dozier, D. A. Roberts, R. E. Davis, and R. O. Green, "Retrieval of subpixel snow-covered area and grain size from imaging spectrometer data," *Remote Sens. Environ.* **85**, 64–77 (2003).
49. T. C. Grenfell, D. K. Perovich, J. A. Ogren, "Spectral albedos of

an alpine snowpack," *Cold Regions Sci. Technol.* **4**, 121–127 (1981).

- 50. C. Sergent, C. Leroux, E. Pougatch, and F. Guirado, "Hemispherical-directional reflectance measurements of natural snow in the 0.9–1.45  $\mu\text{m}$  spectral range: comparison with adding-doubling modelling," *Ann. Glaciol.* **26**, 59–63 (1998).
- 51. T. Aoki, T. Aoki, M. Fukabori, Y. Tachibana, F. Nishio, and T. Oishi, "Spectral albedo observation of the snow field at Barrow," *Polar Meteorol. Glaciol.* **12**, 1–9 (1988).
- 52. T. H. Painter, B. Duval, W. H. Thomas, M. Mendez, S. Heintzelman, and J. Dozier, "Detection and quantification of snow algae with an airborne spectrometer," *Appl. Environ. Microbiol.* **67**, 5267–5272 (2001).
- 53. G. Horneck, "The microbial world and the case for Mars," *Planet. Space Sci.* **48**, 1053–1063 (2000).
- 54. G. Horneck, P. Rettberg, G. Reitz, J. Wehner, U. Eschweiler, K. Strauch, C. Panitz, V. Starke, and C. Baumstark-Khan, "Protection of bacterial spores in space, a contribution to the discussion on panspermia," *Origins Life Evol. Biosphere* **31**, 527–547 (2001).
- 55. S. Marshall and R. Oglesby, "An improved snow hydrology for GCMs. 1. Snow cover fraction, albedo, grain size, and age," *Climate Dynam.* **10**, 21–37 (1994).